A NEW MULTI-STACK POLYPHASE SYNCHRONOUS RELUCTANCE MACHINE

By

L.U. Anih, & E. S. Obe
Department of Electrical Engineering,
University of Nigeria, Nsukka

Abstract

A hybrid polyphase synchronous reluctance machine comprising a cylindrical rotor and a salient pole rotor mechanically coupled together and integrally wound has been reported recently as a high torque device. This paper describes how the hybrid machine can be simulated with only salient pole machines and investigates some performance indices of the machine. The proposed machine comprises three mechanically coupled salient pole machines designated as stacks A, B, C. Each stack machine has two sets of magnetically coupled identical windings star-connected on the stator side, known as the main and control windings respectively. The main windings of each stack are interconnected in series and connected to the utility supply while the control windings are integrally connected and feeds a variable capacitance load. A unique feature of the machine is that although the d-axis to q-axis reactance ratio of the machine is fixed by the geometrical configuration of the rotors, its operational value is dependent on the capacitance loading of the control winding. By the judicious choice of capacitance loading of the control winding, this ratio ranging from 0 to $\pm\infty$ is obtainable, which in turn indicates a great improvement on the output power and power factor of the conventional synchronous reluctance machines.

Key words: *main and control windings, permeance, X_D/X_Q ratio, current and impedance loci, capacitance loading*

1.0 Introduction

Two identical synchronous reluctance machines mechanically coupled together and having their respective windings connected in series phase by phase, and also provided with another set of control windings which are also connected in series phase by phase and short circuited, can start and run as an asynchronous motor and will have a synchronous speed that is half the normal one for the individual machines [2]. The set cannot operate at the synchronous speed unless the short circuit is removed and the control windings fed with dc to provide a stationary field. If one of the machines has a cylindrical rotor, the combination will run as synchronous reluctance machine at the field speed and not requiring dc excitation [3]. A very important feature of this combination is that the effective quadrature axis reactance can be controlled. This is accomplished by varying the value of the reactance load connected to the control windings. This strategy gives a convenient control over the d-axis to q-axis ratio, which determines the reluctance torque magnitude and power factor.

The main objective of this paper is to show how the performance characteristics of a cylindrical rotor machine mechanically coupled to a salient pole machine as stated above can be simulated with only salient pole machines and to assess the performance indices of the machine. The proposed machine can operate as a motor or a generator. The advantages of the machine include the absence of brushes and slip-rings, which connotes minimal maintenance, and good chances of survival in a harsh environment. Furthermore, the proposed machine has the capability of operating the load at a leading or unity power factor by the judicious selection of the capacitance loading of the control winding. Such a machine will be well suited for high speed drives in view of the absence of rotating windings. In the recent times, rekindled interest is being focused on dual winding synchronous reluctance machines having separate polyphase windings housed in the stator for use as motor drives and generator systems [4].

2.0 Description of the machine scheme

The proposed machine comprises three salient pole reluctance machines A, B, C, which are mechanically coupled together such that the rotors of A and B are in space quadrature (i.e. the pole axes of stacks A and B are 90^o displaced from each other in space). The position of the pole axis of stack C with respect to the A-B orthogonal combination is immaterial. Each stack has two sets of identical magnetically coupled windings known as the main and control windings, which occupy the same electrical positions for perfect coupling. The main windings of the component machines are interconnected in series and connected to the utility supply. The control windings of stacks A and B are also connected in series but transposed in stack C section and feeds a balanced capacitance load as shown in Fig. 1. It is shown that the combination of stacks A and B constitutes a cylindrical rotor machine whose synchronous reactance is independent of the rotor angular position. The three-stack machine thus reduces effectively to a cylindrical rotor machine, mechanically coupled to a salient pole machine.

3.0 Impedance of the machine windings

The impedance per unit axial length of stack A machine as a function of the load angle with negligible winding resistance is given by [5,6]:

$$Z_A = j\{\tfrac{1}{2}(X_d+X_q) + \tfrac{1}{2}(X_d-X_q)\,\underline{/2\delta}\}\ldots\ldots\ldots\ldots(1)$$

Therefore, the impedance per unit axial length of stack B, which is 90^o phase displaced from A will be given by:

$Z_B = j\{½(X_d + X_q) + ½(X_d - X_q) \underline{/2(\delta - 90^o)}\}$...(2)

The impedance per unit axial length of the combination machine of stacks A and B will be given by:

$Z_{AB} = Z_A + Z_B = j(X_d + X_q)$ ....(3)

Equation (3) shows that the combined impedance of stacks A and B, Z_{AB}, is independent of the load angle δ and is thus equivalent to a synchronous reactance $jX_s = j(X_d+X_q)$ of a cylindrical rotor machine in magnitude. Suppose this combination machine AB is coupled to a stack C salient pole machine whose d-axis reactance per unit axial length is X_d'.

Therefore, on the d-axis, the effective overall d-axis reactance per unit axial length will be given by: $X_D = X_d' + (X_d + X_q)$...................(4)

And on the q-axis, the effective overall q-axis reactance per unit axial length is:

$X_Q = X_q' + (X_d + X_q)$............................(5)

It is assumed that machines A and B are identical in all respects.

If the synchronous reactance per unit axial length of the combination machine Z_{AB} i.e. $j(X_d + X_q)$ is made equal to the direct axis reactance X_d' of stack C machine that is $(X_d + X_q) = X_d'$ by adjustment of the axial lengths of machines C and A, therefore equations (4) and (5) will reduce to:

$X_D = X_d' + X_d' = 2X_d'$ ....(6)

$X_Q = X_d' + X_q'$ ....(7)

(X_D and X_Q include the effect of leakage fluxes).

The overall X_D/X_Q ratio of the multi-stack machine will be given by:

$$\frac{X_D}{X_Q} = \frac{2X_d'}{X_d' + X_q'} = \frac{2k}{1+k} \quad ....(8)$$

where $k = X_d'/X_q'$ is the saliency factor.

It is shown that the overall X_D/X_Q ratio of the multi-stack machine can be increased and hence the output power if the control winding is capacitively loaded even though X_D/X_Q is fixed by the rotor configuration.

4.0 Equivalent circuit of the multi-stack machine

The impedance of stack C synchronous reluctance machine as a function of the load angle δ is similarly given by:

$Z_C = j\{½(X_d' + X_q') + ½(X_d' - X_q') \underline{/2\delta}\}$.........(9)

The gross impedance of the multi-stack machine is therefore given by:

$$\begin{aligned} Z_{ABC} &= j\{X_d' + ½(X_d' + X_q') + ½(X_d' - X_q') \underline{/2\delta}\} \quad ...(10) \\ &= j[X_d' + ½(X_d' + X_q') \\ &\quad + ½(X_d' - X_q')\{\cos 2\delta + j\sin 2\delta\}] \\ &= j[2X_d' - ½(X_d' - X_q') \end{aligned}$$

$+ \frac{1}{2}(X_d'-X_q')(\cos 2\delta + j\sin 2\delta)]$.....(11)

The equivalent circuit of the machine can be derived from equation (11). The term $j2X_d'$ represents the self-reactance of the main windings whereas $-\frac{1}{2}(X_d'-X_q')+\frac{1}{2}(X_d'-X_q')^*$ $(\cos 2\delta + j\sin 2\delta)$ represents the mutual impedance between the main and control windings. Since the control windings are identical to the main windings, its own self-reactance is also $j2X_d'$. Therefore, the single-phase equivalent circuit of the machine when the control winding feeds a variable capacitance load is as shown in Fig. 2.

4.1 Input Impedance

The input impedance of the machine is given by:

$$\frac{V_1}{I_1} = Z = j\left(2X_d' + \frac{(X_v - X_d')(2X_d' - X_c)}{X_v + X_d' - X_c}\right) \text{..(12)}$$

substituting for X_v, equation (12) becomes equation (13) :

$$Z = j\left(\frac{(4X_d'-X_c)(k-1)\cos 2\delta + (4X_d'-X_c)(k+1) - 2kX_c + j(k-1)(4X_d'-X_c)\sin 2\delta}{3k+1+(k-1)\cos 2\delta - 2k\frac{X_c}{X_d'} + j(k-1)\sin 2\delta}\right)$$

........(13)

where $k = X_d'/X_q'$

Conjugation of equation (13) is rather cumbersome, and the following approach, which is amenable to computer solution, is adopted.

Let $a = (4X_d'-X_c)(k-1)\cos 2\delta + (4X_d'-X_c)(k-1)$
$-2kX_c$ ....(14)

$b = (k-1)(4X_d'-X_c)\sin 2\delta$ ....(15)

$c = 3k+1+(k-1)\cos 2\delta - 2k\{X_c/X_d'\}$..........(16)

and

$d = (k-1)\sin 2\delta$................................(17)

Therefore, equation (13) becomes:

$$Z = \left\{\frac{a+jb}{c+jd}\right\} \text{.....................................(18)}$$

$$= \left[-\left\{\frac{bc-ad}{c^2+d^2}\right\} + j\left\{\frac{ac+bd}{c^2+d^2}\right\}\right] \text{...............(19)}$$

$= -Re + jXe$...(20)

The input impedance of equation (13) and hence the performance indices of the machine can be realized from the equivalent circuit of Fig. 1. and shown in the Appendix.

4.2 Axis reactances of the machine

Consideration of equation (13) leads directly to the direct and quadrature axes reactances of the machine. Thus when $\delta=0$, the rotor is in direct axis position and hence,

$X_D = 2X_d'$ ....(21)

and when the rotor is in the quadrature axis position, $\delta = \frac{1}{2}\pi$, hence,

$$X_Q = \frac{(4X_d'-X_c) - kX_c}{k+1-\frac{kX_c}{X_d'}} \text{.......................(22)}$$

From equations (21) and (22), it is evident that for a fixed value of k, on a base impedance of X_d' that the effective quadrature axis reactance X_Q is a dependent variable on X_c. Thus, variation of X_c varies the quadrature axis reactance while the direct axis reactance remains unaffected.

4.3 Circle diagrams

The impedance loci of equation (20) as δ varies from zero to π for different values of X_c and for a fixed value of k are circles, which are tangential to the point $X_D = 2X_d'$ and of centre: $[0, \frac{1}{2}(X_D+X_Q)]$ and radius $\frac{1}{2}(X_D-X_Q)$.

A plot of equation (20) for k=1.5 and for different values of X_c as δ varies from zero to π on a base impedance X_d' of is shown in Fig. 3a. The current loci, the inverse of the impedance loci will also be circles for a constant applied voltage and tangential to the point $I = V/2X_d'$. The current loci for a unit applied voltage on a base impedance of X_d' for k=1.5 as δ varies from 0 to π is as shown in Fig. 3b for differing values of X_c.

The abscissa of the impedance loci passing through the impedance loci centres (Fig. 3a) mark the transitions between motoring and generating actions and it also applies to the current loci. The maximum power obtainable from each impedance locus is directly proportional to the diameter of the locus. For the locus of infinite radius (locus e) the output power tends to infinity.

4.4 Power factor

The power factor of the machine can be readily deduced from equation (20) as:

$$cos\phi = \frac{-Re}{(Re^2 + Xe^2)^{\frac{1}{2}}} \qquad \text{...........................(23)}$$

A plot of the power factor against δ on a base impedance of X_d' for various values of X_c is shown in Fig. 4. The plot shows an improved power factor up to unity. This improvement is due to the high d-axis to q-axis reactance ratio. The higher the value of this ratio, the better is the performance of a reluctance machine in terms of maximum torque and power factor [5]. For clarity, power factor plots for X_c=1.67 and X_c=1.72 are omitted but their peak values are as indicated in Table 1.

It can be observed that the values of power factor depend on the location of each impedance and current loci from the origin as well as its magnitude. All loci that encircle the origin or tangential to it produce unity power factors.

The expression for the maximum power factor is derived more conveniently by considering the geometry of the circle diagram for the current vector, which is tangential to the current locus as shown in Fig. 5. From Fig. 5, the maximum power factor is given by:

$$cos\phi_{max} = \frac{X_D - X_Q}{X_D + X_Q} = \frac{\frac{X_D}{X_Q} - 1}{\frac{X_D}{X_Q} + 1} \qquad \text{................(24)}$$

where X_D and X_Q are as defined by equations (21) and (22) respectively. Equation (24) emphasizes the importance of large values of this ratio.

5.0 Torque

Consider a cylindrical stator with three-phase windings, which produces constant amplitude rotating mmf. If the rotor has saliency such that the permeance varies symmetrically about two orthogonal axes (*d* and *q*) and the mmf is constant, the magnetic energy stored in the machine will vary with the relative position of the axes of the rotor with respect to that of the mmf. There will be a torque on the rotor equal to the rate of change of stored energy with angular displacement $\left(\frac{\partial W_f}{\partial \delta}\right)$.

Alternatively, the output torque, T, in synchronous watts ignoring losses, is simply given by:

$$T = \frac{3V^2(X_D - X_Q)}{2X_D X_Q} \sin 2\delta \quad \ldots\ldots\ldots\ldots\ldots\ldots\ldots (25)$$

where X_D and X_Q are as defined by equations (21) and (22). A plot of equation (25) for a unit applied voltage, on a base impedance of X_d' for k=1.5 as δ varies from 0 to π for differing values of X_C is shown in Fig. 6. Maximum torque occurs at $\delta=45^o$ generating for $\delta<0$, with maximum torque at $\delta=-45^o$.

6.0 Flux distribution in the machine

When the control windings are on open circuit, the basic characteristics of the machine will be similar to those of the conventional synchronous reluctance machine. Let the airgap permeance distribution in the cylindrical section of the machine comprising stacks A, B, be 'a' and that of the salient pole section stack C (neglecting higher order harmonics) be $a_o+a_1\cos2(\theta-\omega_o t-\delta)$ where ω_o is the angular velocity of the rotor. The excitation mmf distribution is given by $m=M_o\cos(\theta-\omega_o t)$. The airgap flux density distributions in the cylindrical and salient pole sections are respectively:

$$B_1= aM_o\cos(\theta-\omega_o t)\ldots\ldots\ldots\ldots\ldots\ldots\ldots\ldots(26)$$

and

$$B_2 = M_o[a_o + a_1\cos2(\theta-\omega_o t-\delta)]\cos(\theta-\omega_o t)\ldots\ldots(27)$$

The fundamental component of the overall effective flux density distribution will be given by $B_1 + B_2$ as:

$$\begin{aligned}B_o &= M_o\{(a+a_o)\cos(\theta-\omega_o t) \\ &\quad + \tfrac{1}{2}a_1(\cos2\delta\cos(\theta-\omega_o t)) \\ &\quad + \tfrac{1}{2}a_1(\sin2\delta\,\sin(\theta-\omega_o t))\}\ldots\ldots\ldots\ldots(28) \\ &= M_o\{(a+a_o)\cos(\theta-\omega_o t) \\ &\quad + \tfrac{1}{2}a_1(\cos2\delta-j\sin2\delta)\cos(\theta-\omega_o t))\} \\ &= M_o\{(a+a_o) \\ &\quad + \tfrac{1}{2}a_1(\cos2\delta-j\sin2\delta)\}\cos(\theta-\omega_o t)\ldots\ldots\ldots(29)\end{aligned}$$

The primary winding flux as the control winding sees it will be:

$$\begin{aligned}M_{21} &= aM_o\cos(\theta-\omega_o t) \\ &\quad - M_o\{a_o+a_1\cos2(\theta-\omega_o t-\delta)\}\cos(\theta-\omega_o t)) \\ &= M_o\{(a-a_o)\cos(\theta-\omega_o t) - \tfrac{1}{2}a_1\cos(\theta-\omega_o t-2\delta)\} \\ &= M_o\{(a-a_o) \\ &\quad - \tfrac{1}{2}a_1(\cos2\delta-j\sin2\delta)\cos(\theta-\omega_o t)\}\ldots\ldots(30)\end{aligned}$$

The magnitude of the emf induced in the control winding will thus be proportional to $(a-a_o)-\tfrac{1}{2}a_1(\cos2\delta-j\sin2\delta)$.

If $a = a_o + \frac{1}{2}a_1$, which is the necessary and sufficient condition that the synchronous reactance of the stacks A, B, (X_d+X_q) equals direct axis reactance X_d' of the stack C the emf will be zero when $\delta=0^o$. It will be a maximum when $\delta=90^o$. Since the induced emf is zero when the machine is on load ($\delta=0$) and maximum when $\delta=\frac{1}{2}\pi$, which is the range of the stability limit of synchronous machines, the multi-stack machine can be adapted for load angle and synchronous power measurements [7,8].

7.0 Discussion of results

The characteristics of the machine could easily be deduced from the impedance and current loci of Figs. (3a) and (3b) respectively; and those of the torque and power factor by Figs. 5 and 6 respectively in conjunction with Table 1. Each impedance locus has a corresponding current locus as identified by identical letterings on the loci.

When the control winding is on open circuit (X_c being very large), the machine will operate as a normal synchronous reluctance machine. In this mode, the d-axis reactance $X_D=2$ p.u.on a base impedance of X_d' while the quadrature axis reactance X_Q is 1.67 pu. The torque and power factor are very low, 0.15p.u and 0.09 respectively. The device cannot operate or supply any reasonable load in this mode because of the low output power and power factor.

When the control winding is short-circuited ($X_c=0$), the diameter of the impedance locus increases, without changing the direct axis reactance X_D, which remains at 2 p.u, while the quadrature axis reactance X_Q decreases to a new value 1.6 p.u., thereby giving a higher X_D/X_Q ratio over the open circuit case. There is a torque enhancement from 0.15 p.u. to 0.18 p.u and power factor as well, from 0.09 to 0.11 which confirms that the introduction of the short-circuited control windings enhances the output power for a fixed geometrical configuration; since the diameter of the impedance circle is increased.

The introduction of a variable capacitance load into the control winding makes the quadrature axis reactance X_Q variable and can be made to vary from zero to infinity depending on the value of the capacitance load. Some of the loci need special comments.

For Xc=1.6 p.u on the impedance loci locus c), the quadrature axis reactance X_Q is completely neutralized to zero (i.e. $X_Q=0$) by the capacitive reactance while the X_D remains constant at 2 p.u. Hence, the resulting infinite X_D/X_Q (as $X_Q \rightarrow 0$) means that very large and stable synchronous power can be obtained using this scheme. The torque corresponding to this is $3X10^6$ p.u, which to all intents and purposes could be regarded as infinite.

The corresponding power factor is unity. On the current loci, the corresponding locus is a straight line extending to $\pm\infty$. Further increase in X_c between 1.6 p.u. and 1.67 p.u, the machine operates with leading power factor and with reduced output power and power factor. For X_c = 1.64 p.u, the centre of the impedance loci coincides with the origin i.e. $|-X_D| = |X_Q|$. In this mode of operation, the machine will draw or supply the same current irrespective of load and operates as a round rotor synchronous reluctance machine irrespective of the magnetic circuit saliency.

For X_c=1.67 p.u., X_Q is infinite and the corresponding current locus is I_Q=0. In this mode, the machine will operate as an ideal synchronous reluctance machine drawing a negligible amount of input current for its operation and no losses.

For X_c>1.67 p.u, the impedance loci flip over to the right hand side of the $X_Q=\infty$ (locus e) with X_Q becoming greater than X_D which implies that the operating axis of the machine has shifted by ½π radians, the q-axis becoming the no-load axis. The torque–angle curve of the machine will flip to the right hand side about the abscissa axis thus becoming negative for motoring action and positive for generator operation as indicated by curves f and g of Fig 6. The shrinking of the flipped impedance loci is because the capacitive reactance is now becoming very large and thus increasing the impedance of the control winding circuit. The effect is that the current in the control winding decreases. The inductive nature of the impedance in this mode is consistent with the analytical predictions because, the overall impedance of the machine is now returning to the open circuit condition, which is inductive in nature.

The impedance loci are tangential to the straight line passing through X = j2 p.u while the current loci are tangential to the straight line passing though I_r=j0.5 p.u.

When the value of X_c equals that of the effective d-axis reactance in magnitude (i.e. X_c=2p.u), the d-axis reactance and q-axis reactance coincide at tne same point located at (2.0, 0) as a dot, which is a circle of zero radius. Consequently, the output power and power factor are zero.

It is of importance to note that the values of X_c giving higher torques also give higher power factors. If the winding resistances were not negligible, the effect will be merely to raise all the curves slightly by an amount proportional to the winding resistance.

8.0 Conclusions

It has been shown that the performance characteristics of a cylindrical rotor machine mechanically coupled to a salient pole machine can be simulated with three salient pole machines only. The machine can be operated as a motor or a generator. In both operating modes, the machine will be connected to an existing supply for the purpose of deriving its magnetizing current like an induction generator. The machine will require squirrel cage windings on its rotors if it is to run up by itself as a motor. The cage acts as a damper and (for fixed frequency operation) to provide the asynchronous (induction motor) torque to start the machine and raise the speed to a value from which reluctance torque can provide synchronous pull-in. At the synchronous speed, the rotor windings become redundant except for the purpose of damping out transient torques. As a generator, it will require rotor windings with dc excitation if it will operate as a stand alone or isolated synchronous reluctance machine.

The impedance and current loci of the machine show that while the d-axis reactance is constant, the q-axis reactance varies between zero and infinity. The high output power is at good power factor and hence less current. When the q-axis reactance approaches infinity, that is a circle with infinite radius, the corresponding current, I_Q will approach zero and the machine operates with negligible input current. In this mode of operation, the machine will be operating as an ideal synchronous reluctance machine. In view of the high output power capability of the machine arising from the ultra-high X_D/X_Q ratio, the machine has a strong potential for bulk power generation. Good load synchronization can be assured by adjusting the X_D/X_Q ratio for optimum pull-in torque and subsequently raising it for high pull-out torque and load stability.

9.0 References

1. L. A. Agu and L. U. Anih "Enhancement of the output power of synchronous reluctance machines by capacitance injection technique" *Accepted for publication in the Technical Transactions of the Nigerian Society of Engineers. May 2002.*

2. L. A. Agu, "Transfer-field electric machines" *Journal of Electrical Machines and Electromechanics* Vol.2 No. 4, 1978 pp. 403-418

3. L. A. Agu and L. U. Anih, "A variable X_q synchronous reluctance machine" *Proc. Electric Power Engineering Conference (EPEC),* Nsukka, Dec. 1997, pp.48-53

4. O. Ojo and Z. Wu , "Synchronous operation of dual winding reluctance generator" Accepted for publication in the *IEEE Trans. on Energy Conversion*, PE-464-EC0-01-1997

5. P. J. Lawrenson and L. A. Agu "Theory and performance of polyphase reluctance machines" *Proc. IEE,* Vol. III No. 8, Aug. 1964, pp.1435-1445.

6. A. T. Morgan, "*General Theory of electrical machines*" *London: Heyden and Sons Ltd, 1979 p.199*

7. L. A. Agu and E. S. Obe " A novel device for the measurement of load angle of synchronous machines" *Proc. Intl. Electric Power Engineering Conference (IEPEC), University of Nigeria, Dec. 1997.* pp. 64

8. L. A. Agu and E. S. Obe " A new method of measuring power in synchronous machines" *Proc. Electric Power Engineering Conference (EPEC),* Nsuka, Mar. 1999. pp. 46.

10.0 Appendix

The coupled equivalent circuit of Fig. 1

It is set forth in this section to show that Fig. 1 and Fig. 2 are equivalent circuits. Corollary, that the input impedance of equation (13) can be realized with the coupled circuit equivalent of the multi-stack machine of Fig. 1. It has been shown in equation (3) that the impedance of stacks A, B whose rotor are orthogonal in space is equivalent to a cylindrical rotor machine whose synchronous reactance is $j(X_d+X_q)$. It was further stated that this impedance $Z_{AB}= j(X_d+X_q)$ can be made equal to the direct axis reactance X'_d of stack C machine by the adjustment of the axial lengths of stack C machine and that of stack A, which is identical stack B. The three-stack machine thus reduces to a two-stack machine whose equivalent circuit is as shown in Fig. A. Fig. B shows the connection diagram of the three salient pole machines.

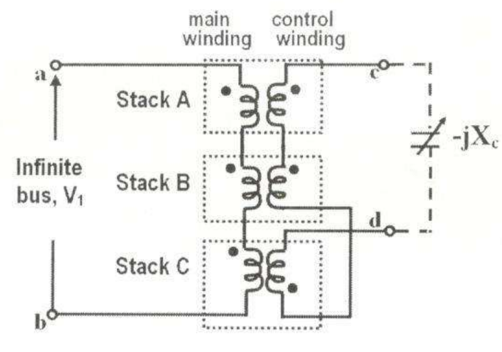

Fig.1: The connection diagram of the multi-stack machine

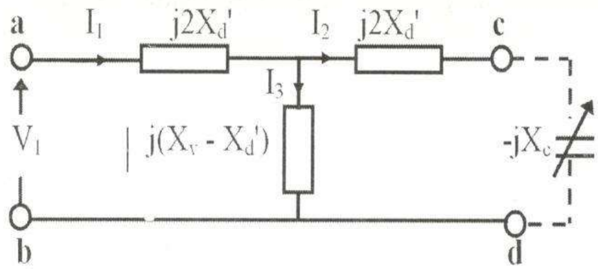

$X_v = j\{½(X_d'+X_q') + ½(X_d'-X_q')(\cos 2\delta + j\sin 2\delta)\}$

Fig.2: The per phase equivalent circuit of the multi-stack machine

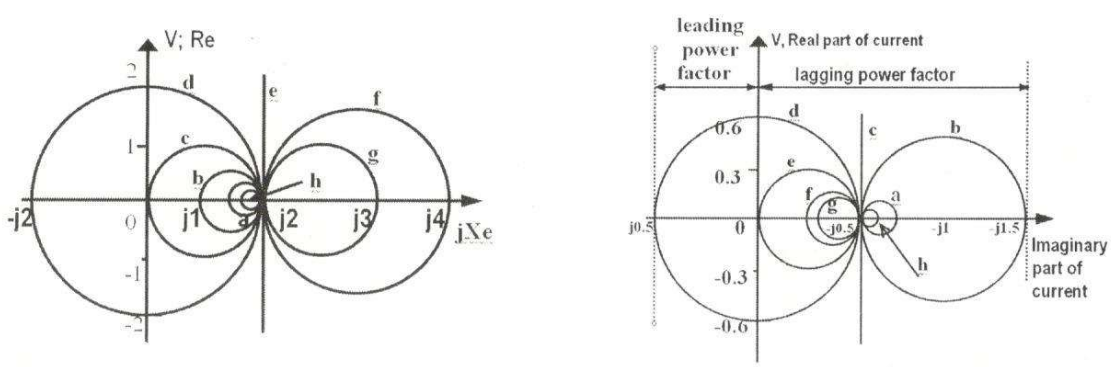

(a) (b)

Fig. 3: Loci of the multi-stack machine (a) impedance and (b) current

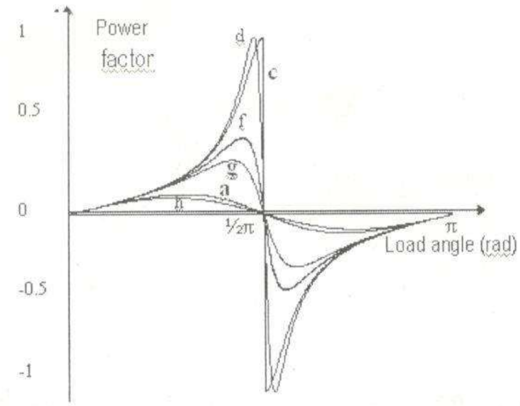

Fig 4: Power factor - angle plots of the multi-stack machine

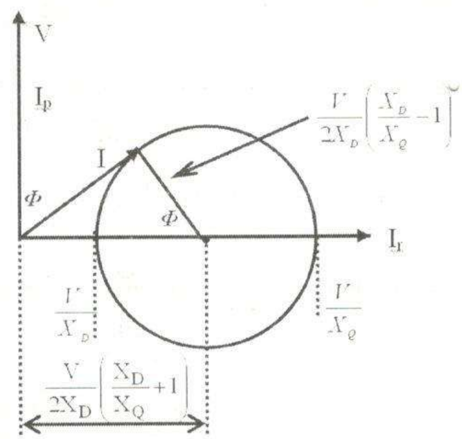

Fig. 5: Schematic input current locus

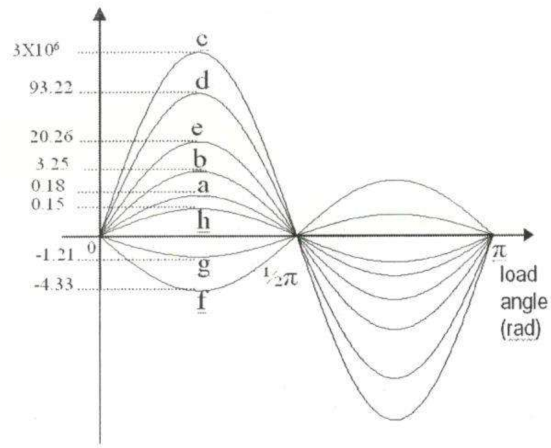

Fig. 6: Torque-angle plots for different values of X_c

Table 1: Glossary to the plots

Loci	Value of X_c in p.u of X_d'	Pull-out torque (p.u)	Power factor
a	0	0.18	0.11
b	1.54	3.25	0.42
c	1.60	$3X10^6$	1.0
d	1.64	93.22	1.0
e	1.67	20.26	1.0
f	1.72	-4.33	0.41
g	1.74	-1.21	0.36
h	∞	0.15	0.09

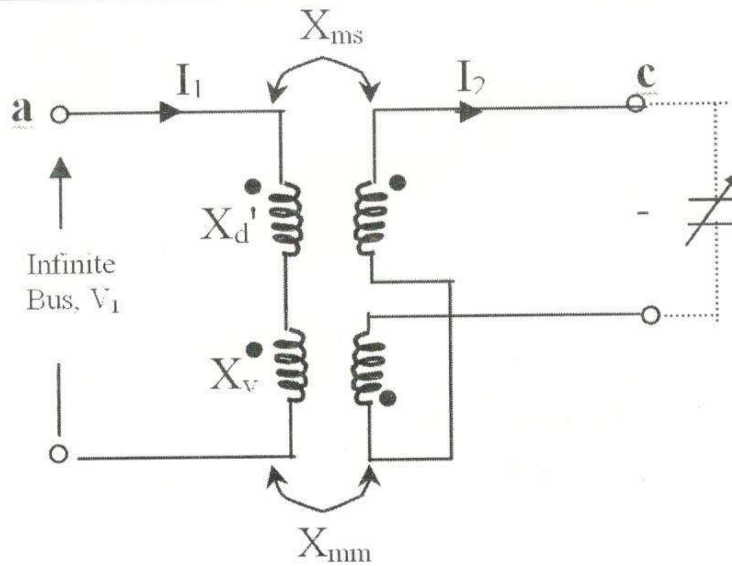

$X_v = j\{\tfrac{1}{2}(X_d'+X_q') + \tfrac{1}{2}(X_d'-X_q')(\cos 2\delta + j\sin 2\delta)\}$
$\quad = j\{X_o + X_1(\cos 2\delta + j\sin 2\delta)\}$

Fig A: Coupled equivalent circuit

Looking through terminals a - b

$V_1 = jI_1X_d' - jI_2X_{ms} + jI_1X_v + jI_2X_{mm}$ ....(31)

For perfect coupling $X_{ms}= X_d'$ and $X_{mm}= X_v$

Therefore,

$V_1 = jI_1X_d' + jI_1X_v - jI_2X_d' + jI_2X_v$ ....(32)

$\quad = jI_1(X_d' + X_v) + jI_2(X_v - X_d')$ ....(33)

Looking through terminals c – d

$I_2X_c = I_2X_v + I_1X_{mm} + I_2X_s - I_1X_{ms}$ ....(34)

Assuming perfect coupling again,

$I_2X_c = I_2X_v + I_1X_v + I_2X_d' - I_1X_d'$ ....(35)

Therefore,

$I_1(X_d'-X_v) = I_2(X_v + X_d' - X_c)$ ....(36)

and

$$I_2 = \frac{I_1(X_d'-X_v)}{(X_v + X_d' - X_c)} \quad \text{.............................(37)}$$

substituting the value of I_2 in equation (33)

$$V_1 = I_1(Xd'+Xv) + I_1\frac{(X_d'-X_v)(X_v - X_s)}{(X_v + X_d' - X_c)} \quad \text{...(38)}$$

$$\therefore Z = \frac{V_1}{I_1} = \left(\frac{(X_d'+X_v)(X_v + X_d' - X_c) - (X_v - X_d')^2}{(X_v + X_d' - X_c)}\right) = \frac{(4X_d'-X_c)X_v - X_d'X_c}{X_v + X_d' - X_c} \quad \text{.....................(39)}$$

$$= \frac{(4X_d'-X_c)(X_o + X_1(\cos 2\delta + j\sin 2\delta)) - X_d'X_c}{X_o + X_1(\cos 2\delta + j\sin 2\delta) + X_d' - X_c} \quad \text{....(40)}$$

$$= \frac{(4X_d - Xc)X_1\cos 2\delta + (4X_d - X_c)X_o - X_d'X_c + jX_1(4X_d - X_c)\sin 2\delta}{(X_d'+X_o + X_1\cos 2\delta - X_c) + jX_1\sin 2\delta} \quad \text{.............................(41)}$$

$$= \frac{(4X_d'-X_c)\left(\frac{X_d'-X_q'}{2}\right)\cos 2\delta + (4X_d'-X_c)\left(\frac{X_d'+X_q'}{2}\right) - X_d'X_c + (4X_d'-X_c)\left(\frac{X_d'-X_q'}{2}\right)\sin 2\delta}{\left\{X_d' + \left(\frac{X_d'+X_q'}{2}\right) + \left(\frac{X_d'+X_q'}{2}\right)\cos 2\delta - X_c\right\} + j\left(\frac{X_d'-X_q'}{2}\right)\sin 2\delta} \quad \ldots(42)$$

$$Z = j\left(\frac{(4X_d'-X_c)(k-1)\cos 2\delta + (4X_d'-X_c)(k+1) - 2kX_c + j(k-1)(4X_d'-X_c)\sin 2\delta}{3k+1+(k-1)\cos 2\delta - 2k\frac{X_c}{X_d'} + j(k-1)\sin 2\delta}\right) \quad \ldots\ldots\ldots\ldots\ldots(43)$$

Equation (3) is the same as equation (43). This implies that the two circuits are the same as set forth to show.

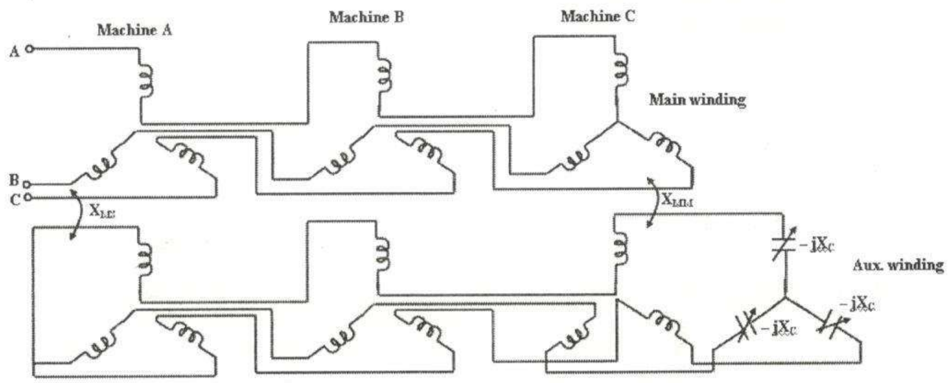

Fig. B: Connection diagram of the three salient pole machines

Nomenclature of per-phase parameters

X_d –d-axis reactance per unit axial length of stack A machine which is same for stack B.
X_d' – d-axis reactance per unit axial length of stack C machine
X_D – effective d-axis reactance per unit axial length of the multi-stack machine (i.e. stacks A, Band C)
X_q – q-axis reactance per unit axial length of stack A machine which is same for stack B
X_q' – q-axis reactance per unit axial length of stack C machine
X_Q – effective d-axis reactance per unit axial length of the multi-stack machine (i.e. stacks A, Band C)
I_1 – input current to the multi-stack machine
k – saliency factor, defined by X_d'/X_q'
V_1 – input voltage to the multi-stack machine
R_e – real part of the input impedance
X_e – imaginary part of the input impedance
X_c – capacitive reactance loading of the auxiliary winding
X_{ms} – mutual coupling reactance in the simulated round rotor section of the multi-stack machine
X_{mm} – mutual coupling reactance in the salient pole section of the multi-stack machine
Z – input impedance of the multi-stack machine defined by V_1/I_1
Z_A, Z_B, Z_C – input impedance per unit axial length of stacks A, B and C machines, respectively.
Z_{AB} – combined impedance per unit axial length of stacks A and B machines
Z_{ABC} – combined per unit axial length of stacks A, B and C machines
δ - electrical load angle of the multi stack machine
φ – power factor angle